Advance Sustainable Science, Engineering and Technology (ASSET)
Vol. 8, No.2, April 2026, pp. 02602031-01 ~ 02602031-013
ISSN: 2715-4211 DOI: https://doi.org/10.26877/asset.v8i2.2401

Comparative Stress Analysis of Balanced Cantilever Bridges Using MIDAS Civil Based on AASHTO, Eurocode, and IRC

Priesta S. Hutagalung, Tavio*

Department of Civil Engineering, Institut Teknologi Sepuluh Nopember, Sukolilo, Surabaya 60111, East Java, Indonesia

*tavio@its.ac.id

Abstract. Evaluating stress behavior in prestressed concrete girders during staged construction is important for structural safety. This study compares stress responses based on three design codes: AASHTO, Eurocode, and IRC. A total of 21 construction stages were simulated using MIDAS Civil 2023 to model a balanced cantilever bridge. The analysis included time-dependent effects such as creep, shrinkage, and prestress losses, following each code's assumptions. To ensure fair comparison, material properties, geometry, and environmental conditions were kept uniform. Results show that the highest compressive stress at the top fiber occurred in the Eurocode model (11,960 kPa), while the highest tensile stress was found in the IRC model (841.3 kPa). At the bottom fiber, IRC also produced the highest compressive (18,630 kPa) and tensile stresses (1,282 kPa). These differences indicate variations in how each code accounts for viscoelastic behavior and stress redistribution. This study highlights the importance of developing a national design standard in Indonesia that balances safety and efficiency by adapting insights from international codes.

Keywords: AASHTO, Balanced Cantilever Bridge, Eurocode, IRC, Prestressed Concrete, Sustainable Infrastructure

(Received 2025-07-19, Revised 2025-08-01, Accepted 2026-08-02, Available Online by 2026-04-30)

1. Introduction

In the bridge planning process, the use of standards or design codes is essential to ensure safety and performance. Various international standards, such as AASHTO-LRFD in the United States, Eurocodes in Europe, and IRC in India, are regularly updated to keep pace with advancements in materials, construction techniques, and infrastructure demands. In the United States, bridge engineers typically follow the AASHTO code, while India and several South Asian countries utilize the IRC (Indian Road Congress) standards. Countries like Germany and the United Kingdom have developed national systems based on the DIN and BS codes, respectively [1]. Among these, the AASHTO standard has gained wide

international adoption due to its clarity, adaptability, and integration of reliability-based design principles [2].

Indonesia, however, currently lacks a comprehensive national design code that specifically addresses segmental bridge construction using balanced cantilever methods. As a result, engineers and consultants often rely on foreign standards, primarily AASHTO, Eurocode, or IRC, without clear guidance on how to adapt them to Indonesia's tropical climate, construction practices, or material behavior. This regulatory gap has the potential to affect safety margins and cost efficiency in large infrastructure projects.

Balanced cantilever bridges are commonly used for medium- to long-span bridge construction, particularly in challenging terrains such as deep valleys or over active transport corridors. Their application minimizes the need for temporary falsework and reduces environmental and traffic disruption below the deck. Although AASHTO LRFD, Eurocode, and IRC each provide guidelines for segmental construction and prestressing, variations in load combination, partial safety factors, modeling of time-dependent effects, and construction stage considerations can lead to different structural behaviors and cost implications for the same bridge configuration.

The need for a comparative analysis is especially urgent today, given the increasing number of long-span infrastructure projects under Indonesia's National Strategic Projects (Proyek Strategis Nasional – PSN) and the ongoing revisions to the Indonesian National Standard (SNI) for bridges. Engineers lack a unified local framework to model creep, shrinkage, and prestress loss accurately during staged construction, leading to uncertainty in code selection and design interpretation.

To address these differences, Finite Element Method (FEM) software, such as MIDAS Civil, provides robust tools for modeling construction sequences and simulating time-dependent phenomena, including creep, shrinkage, and prestress loss [3, 4]. This paper conducts a comparative construction stage analysis of a balanced cantilever bridge based on the three aforementioned standards. The simulations aim to capture differences in stress development, particularly at critical top and bottom fiber locations, throughout a staged erection process involving 21 segments.

The problem addressed in this study is the lack of clarity on how different international design codes influence the structural response of segmental bridges during construction. This leads to the following hypothesis: the stress behavior of segmental girders under staged construction differs significantly depending on the modeling assumptions, especially in the treatment of time-dependent concrete properties prescribed by each code. The results of this comparative analysis are expected to support engineers and policymakers in developing or improving Indonesia's national bridge design guidelines, informed by best practices from international standards.

1.1. Literature Review

Several previous studies have already conducted comparisons between design codes from different countries. The literature reviewed primarily focuses on bridge loading conditions, bridge design practices across various standards, and prior research in comparable fields. Seni [5] conducted a comparative analysis of live load specifications in highway bridge designs between North America and Western Europe. His findings indicated that while the loading patterns differ, the magnitudes of the live loads prescribed by the AASHTO and the French standards are quite similar. Thomas [6] formulated a simplified loading model for the structural design of highway bridges in India, integrating current traffic load characteristics with projections of future traffic demand.

Agarwal and Cheung [7] proposed a truck load model and a live load factor of 1.6 for the CSA-S6 bridge design code, adopting a Canadian Standard design truck with a gross weight of 600 kN (CS-600). Structural responses were examined on simply supported bridge spans, and the adequacy of the proposed live load factor was also evaluated for application to continuous span bridges. Bhat [8] introduced a tailored loading framework for highway bridge design in Nepal, addressing the absence of a nationally established standard. In practice, Nepalese engineers typically adopt foreign codes, such as AASHTO and IRC. However, despite being considered equivalent within the Nepal Road Standard, these design approaches often result in bridge capacities that differ by over 50% in numerous cases.

Buckle [9] performed a comparative analysis of seismic design methodologies for highway bridges implemented in several countries, focusing on the fundamental principles and procedural differences across regions such as Europe, Japan, New Zealand, and the United States. Wacker and Groenier [10] conducted a comparative study of timber bridge design standards from Canada, the United States, and Europe. Their analysis explored key elements including code structure, types of superstructures, loading assumptions, material requirements, design criteria for bending and shear, deflection control, and durability considerations.

Okahara et al. [11] performed a comparative evaluation of bridge design standards, focusing on the AASHTO LRFD and European Union codes. Buckland and Sexsmith [12] carried out an assessment of highway bridge design loads by examining the impact of different live load models over span lengths varying from 30 to 300 meters. Raina [13] outlined a practical methodology for the design of concrete bridges, integrating essential structural analysis concepts with applicable design techniques. The study emphasizes various loads and forces relevant to bridge design, including dead and live loads, dynamic impacts from traffic, braking forces, wind, seismic activity, temperature variations, and other influencing factors.

Rajagopalan [14] carried out a global comparison of design loads applied in highway bridge engineering. Given that several countries categorize load specifications according to bridge types, the analysis was limited to examining the design loads prescribed for major bridge structures. Kamal [15] performed a comparative evaluation of bridge design methodologies outlined in the AASHTO Standard and British Codes. The findings suggest that the American standard presents a feasible alternative to the British approach for seismic bridge design applications in Malaysia. Aziz and Ma [16] carried out a comparative study on bridge foundation design subjected to railway loading, utilizing four different standards: AASHTO, British Standard (BS), Chinese National Standard (CNS 2002), and the Chinese Railway Code (TB 10002.5-2005). Their investigation emphasized manual calculations to assess both settlement limitations and the ultimate vertical load capacity of individual piles. Kamde et al. [17] conducted a comparative analysis of single-span bridge design using two design codes, AASHTO LRFD and the Indian Standard Method. The study compared bridge design using AASHTO LRFD and Indian Standards for a 10-meter single-span bridge. Nielsen and Schmeckpeper [18] conducted comparative designs of a single-span AASHTO Type III girder bridge under the AASHTO Standard Specification for Highway Bridges, 16th Edition, and the AASHTO LRFD Bridge Design Specification.

2. Method

This paper aims to conduct a comparative construction stage analysis of balanced cantilever bridges by evaluating the differences in stress responses based on AASHTO, Eurocode, and IRC standards, using simulations implemented in MIDAS Civil. The subject of the study is a balanced cantilever bridge with a main span between gridlines P11 and P14, consisting of a 150-meter central span and two side spans of 89.550 meters each, as shown in Figure 1.

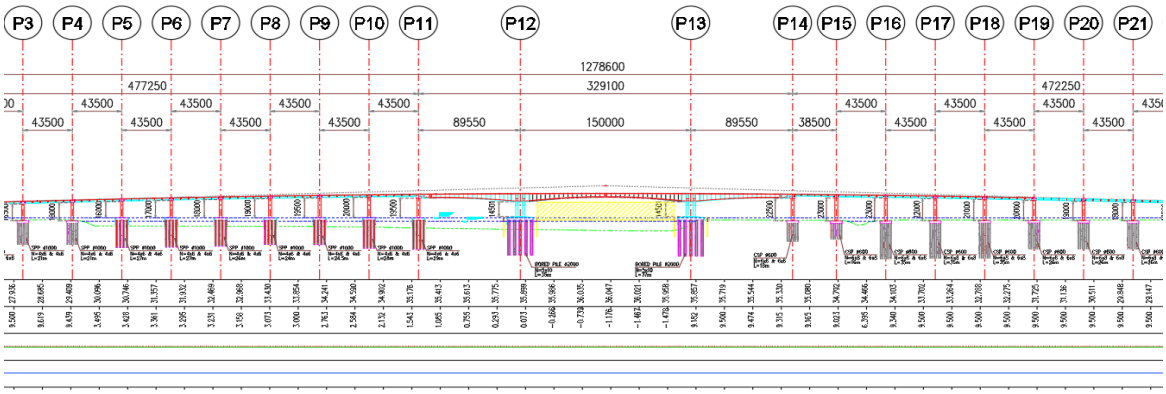

Figure 1. Longitudinal Profile Balanced Cantilever Bridge

The structural modeling was carried out using Midas Civil software with a finite element method approach. The model was developed with uniform geometric parameters, material properties, and support conditions to ensure a consistent basis for comparison. The main span consists of 17 segments, while the side span consists of 18 segments. The segment distribution can be seen in Figures 2 and 3.

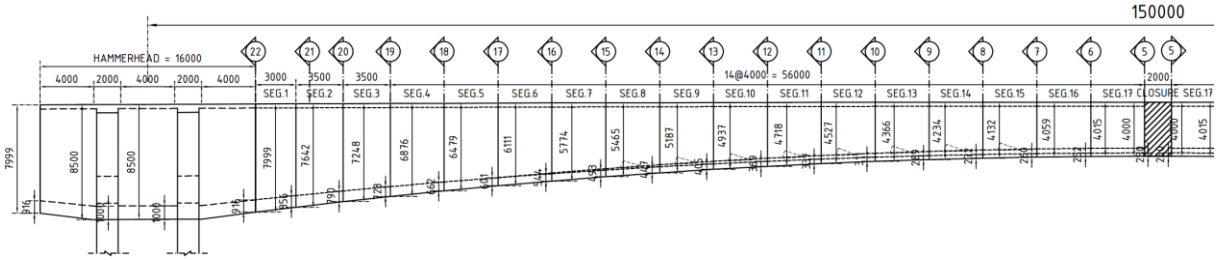

Figure 2. Main Span

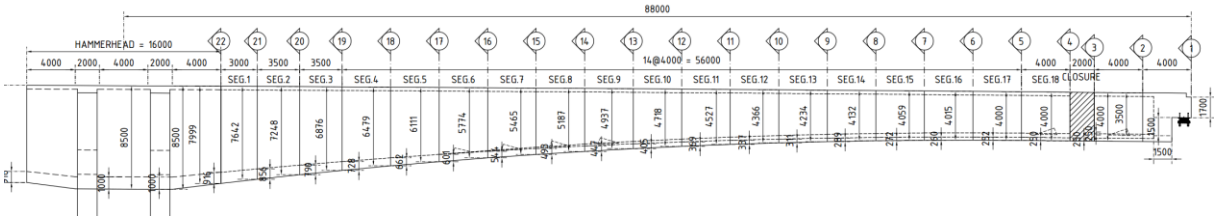

Figure 3. Side Span

The finite element model was discretized using 3D beam elements (Elastic Beam Type) for the superstructure, with mesh refinement concentrated near segment joints and cantilever tips to improve stress accuracy. Each segment was modeled with an element length of 1 meter, ensuring sufficient resolution without compromising computational efficiency. Boundary conditions included fully fixed supports at pier bases and temporary fixed supports (shoring) during early stages, which were deactivated as construction progressed. Bearings were modeled as pinned connections where relevant to allow rotation but restrict horizontal and vertical movement.

In all three models, default material libraries in MIDAS Civil were not used. Instead, custom material inputs were defined for each code based on published parameters in the respective standards. This included explicit input of creep coefficients, shrinkage strains, elastic modulus, and age-dependent properties based on the selected concrete grade and cement type. The approach ensured uniformity of environmental conditions while reflecting the calculation methods prescribed by AASHTO, Eurocode, and IRC.

The construction stage loads in the balanced cantilever bridge model include wet concrete load, tendon load, creep and shrinkage effects, and traveler load.

2.1. Wet Concrete Load

The wet concrete load is applied to the model with each segment addition and during the casting of each new segment. The wet concrete load applied per segment can be seen in Table 1.

Table 1. Loading of wet concrete

Segment	Length (m)	Height (m)		Weight (kN)
		Initial (I)	Joint (J)	
Pier Table	4.00	8.50	8.00	-
Seg1	3.00	8.00	7.64	1686.16
Seg2	3.50	7.64	7.25	1901.27
Seg3	3.50	7.25	6.88	1833.47
Seg4	4.00	6.88	6.48	2017.00
Seg5	4.00	6.48	6.11	1938.44
Seg6	4.00	6.11	5.77	1865.45
Seg7	4.00	5.77	5.47	1798.17
Seg8	4.00	5.47	5.19	1736.77
Seg9	4.00	5.19	4.94	1681.39
Seg10	4.00	4.94	4.72	1632.21
Seg11	4.00	4.72	4.53	1589.38
Seg12	4.00	4.53	4.37	1553.06
Seg13	4.00	4.37	4.24	1523.40
Seg14	4.00	4.24	4.13	1500.56
Seg15	4.00	4.13	4.06	1484.71
Seg16	4.00	4.06	4.02	1476.00
Seg17	4.00	4.02	4.00	1474.59
Seg18	4.00	4.00	4.00	1474.59
Closure	2.00	4.00	4.00	739.08

2.2. Form Traveler Load

In the finite element modeling conducted using MIDAS Civil, the form traveler is modeled to support a construction load of 9 tons (900 kN), applied at the free end of the cantilever segment during each erection stage. This load simulates the weight of construction equipment and platforms used during the segment.

2.3. Creep and Shrinkage

For the design of a balanced cantilever, the construction stage and time-dependent material properties of concrete must be defined. The input method for the concrete's time-dependent properties section material information is presented in the following subsection.

2.3.1 AASHTO

To account for time-dependent effects such as creep and shrinkage during the construction stage analysis, the concrete material was defined in accordance with the CEB-FIP Model Code 2010. Key input parameters include a characteristic compressive strength of 50 MPa, 70% relative humidity, and a notional size of 1 meter. The cement type selected was 32.5 R and 42.5 N, and the onset of shrinkage was assumed at 3 days. Aggregates were modeled as basalt and dense limestone, known for their high stiffness, contributing to reduced long-term deformation. These parameters were implemented in MIDAS Civil to estimate prestress losses, vertical deflections, and internal force redistribution caused by concrete's viscoelastic behavior [19-21].

Model validation was performed by cross-checking the stress development trends against existing literature benchmarks [3, 13] and manually computed sectional stress values at critical stages (Stage 10 and Stage 21). The results showed a deviation of less than 5% between the numerical simulation and reference values, confirming that the model captures the essential structural behavior during construction stages. No field monitoring data were available; hence, literature-based calibration was adopted to confirm model reliability.

2.3.2 EUROCODE

Time-dependent effects of concrete, such as creep and shrinkage, were also modeled according to the European Code, specifically referring to EN 1992-2 (Concrete Bridge). The key parameters included a characteristic cylinder compressive strength of 50 MPa, 70% ambient relative humidity, and a notional member size of 1 meter. The cement type selected was Class N (Normal Hardening Cement), and the onset of shrinkage was set at 3 days. The use of silica fume was not activated in this analysis. This modeling approach aims to provide a more accurate prediction of long-term deformation behavior during the construction stages of segmental bridge erection using the *balanced cantilever method* [22, 23].

2.3.3 IRC Code

In addition to the European and CEB-FIP standards, the time-dependent behavior of concrete due to creep and shrinkage was also modeled in accordance with the Indian standard IRC:112-2011. The main parameters defined in the model were characteristic compressive strength of 50 MPa, ambient relative humidity of 70%, and a notional member size of 1 meter, calculated based on the ratio of section area to the perimeter in contact with the atmosphere. The cement type was set as normal cement, and the age of concrete at the beginning of shrinkage was defined as 3 days. This configuration was employed to represent long-term deformation more accurately, particularly in the segmental bridge construction stages using the *balanced cantilever method*, in accordance with Indian design practice [24-27].

2.4. Tendon

While tendon relaxation effects were mentioned in each code section, a consistent relaxation loss of 5% was assumed across all models, in accordance with standard design recommendations for low-relaxation strands. MIDAS Civil applies this loss automatically during staged prestressing. Although the Eurocode and AASHTO allow refined time-step integration of relaxation effects, this study adopted a unified fixed-loss approach to enable fair comparison across standards. The impact of relaxation on stress redistribution was incorporated indirectly through the adjusted effective prestress force applied at each construction stage.

The longitudinal tendons consist of 66 top tendons, each comprising 22 strands of 0.6". In the side spans, four bottom tendons are used, each with 22 strands of 0.6", while in the main span, eight bottom tendons are provided, also with 22 strands of 0.6" each. The transverse tendons utilize 4 strands of 0.6" with a spacing of 500 mm.

Although this study focused on baseline simulations using a fixed humidity of 70% and standard cement types (e.g., Type I / Class N / 32.5 R), a limited sensitivity check was performed to assess the effect of humidity variation. A 10% increase and decrease in relative humidity altered the total shrinkage strain by up to 15% in Eurocode, 10% in AASHTO, and 8% in IRC. However, these sensitivity results were not plotted in the main analysis to maintain clarity of comparison. Future work should expand this into a full parametric analysis that includes variations in temperature, curing duration, and cement composition to evaluate robustness under different environmental conditions.

2.5. Construction Stage

In the first stage, the foundation elements, pile cap, pier, and box section of the pier table segment are activated. Subsequently, tendon stressing is carried out according to the considered concrete age. Afterward, the structure is subjected to the load from the form traveler and the self-weight of the wet concrete of segment 1. The construction stages of the balanced cantilever method are detailed in Table 2.

Table 2. Construction stage

Stage	Element Activation	Support Activation	Load Activation	Load & Support Deactivation
Stage 1	Pile, pile cap, pier, and pier table	Fix support on the pier, shoring pier table	Self-weight, PS pier table, FT pier table, WC Seg.1	
Stage 2	Seg. 1	Fix support	PS Seg.1, FT Seg.1, WC Seg.2	FT pier table, WC Seg.1, Shoring
Stage 3	Seg. 2	Fix support	PS Seg.2, FT Seg.2, WC Seg.3	FT Seg.1, WC, Seg.2
Stage 4	Seg. 3	Fix support	PS Seg.3, FT Seg.3, WC Seg.4	FT Seg.2, WC, Seg.3
Stage 5	Seg. 4	Fix support	PS Seg.4, FT Seg.4, WC Seg.5	FT Seg.3, WC, Seg.4
Stage 6	Seg. 5	Fix support	PS Seg.5, FT Seg.5, WC Seg.6	FT Seg.4, WC, Seg.5
Stage 7	Seg. 6	Fix support	PS Seg.6, FT Seg.6, WC Seg.7	FT Seg.5, WC, Seg.6
Stage 8	Seg. 7	Fix support	PS Seg.7, FT Seg.7, WC Seg.8	FT Seg.6, WC, Seg.7
Stage 9	Seg. 8	Fix support	PS Seg.8, FT Seg.8, WC Seg.9	FT Seg.7, WC, Seg.8
Stage 10	Seg. 9	Fix support	PS Seg.9, FT Seg.9, WC Seg.10	FT Seg.8, WC, Seg.9
Stage 11	Seg. 10	Fix support	PS Seg.10, FT Seg.10, WC Seg.11	FT Seg.9, WC, Seg.10
Stage 12	Seg. 11	Fix support	PS Seg.11, FT Seg.11, WC Seg.12	FT Seg.10, WC, Seg.11
Stage 13	Seg. 12	Fix support	PS Seg.12, FT Seg.12, WC Seg.13	FT Seg.11, WC, Seg.12
Stage 14	Seg. 13	Fix support	PS Seg.13, FT Seg.13, WC Seg.14	FT Seg.12, WC, Seg.13
Stage 15	Seg. 14	Fix support	PS Seg.14, FT Seg.14, WC Seg.15	FT Seg.13, WC, Seg.14
Stage 16	Seg. 15	Fix support	PS Seg.15, FT Seg.15, WC Seg.16	FT Seg.14, WC, Seg.15
Stage 17	Seg. 16	Fix support	PS Seg.16, FT Seg.16, WC Seg.17	FT Seg.15, WC, Seg.16
Stage 18	Seg. 17	Fix support	PS Seg.17, FT Seg.17 (L/R), Closure mid span	FT Seg.16, WC, Seg.17
Stage 19	Closure mid-span	Fix support	PS Closure mid span, FT Seg.17 (L/R), WC Seg.18	WC Closure mid span
Stage 20	Seg. 18 & FSM	Fix support & shoring FSM	PS Seg.18, FT Seg.18 (L), FT Seg.17 (R), Closure side span	WC Seg.18
Stage 21	Closure side span	Fix support & roll FSM	PS closure side span	FT Seg.18 (L), FT Seg.17 (R), WC Closure side span & Shoring FSM
Stage 22	Creep Shrinkage 10000 days			

Note: Seg. = Segment PS= Prestress FT=Form Traveler WC= Wet Concrete

3. Results and Discussion

The stage construction analysis model is employed to evaluate the time-dependent structural response throughout each phase of the construction sequence. This includes the effects of stress redistribution

resulting from the removal of temporary supports (scaffolding), the sequential addition of cantilever segments, and the application of time-dependent factors such as creep, shrinkage, and tendon prestressing. This method allows for a more realistic simulation of the construction process and is essential for capturing the progressive behavior and internal force development in segmental balanced cantilever bridges.

3.1. Stress Comparison During the Construction

The stage construction analysis model is used to evaluate the structural response at each phase of stress redistribution due to the removal of formwork and the sequential addition of segments. The segmental stress response of the balanced cantilever model during construction for the three design standards is presented in Figures 4 and 5.

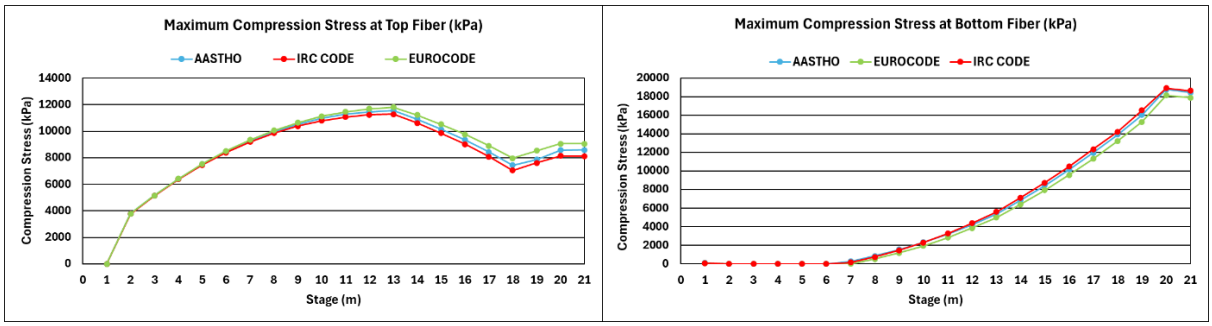

Figure 4. Maximum Compression Stress Distribution at Top and Bottom Fibers During Staged Construction (Stages 1–21) at Midspan

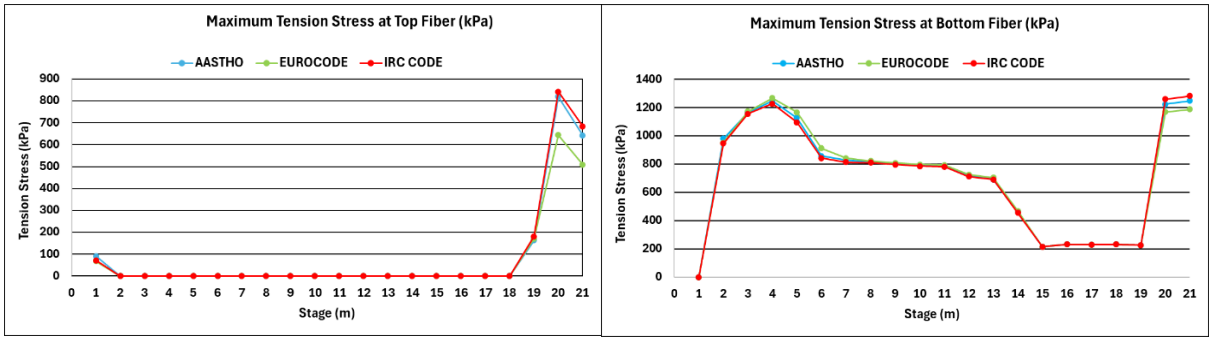

Figure 5. Maximum Tension Stress Distribution at Top and Bottom Fibers During Staged Construction (Stages 1–21) at Midspan

Figures 4 and 5 illustrate the stress development in the top and bottom fibers at the midspan during each construction stage. The vertical axis represents stress magnitude in kilopascals (kPa), while the horizontal axis denotes the construction stage (1 to 21). Each line represents a different code: AASHTO (blue), Eurocode (green), and IRC (red). The graphs exclude color bars since they represent line charts; however, all values were extracted from MIDAS Civil stress output at control nodes. The plots confirm consistent trends across all codes, though the magnitude and rate of stress accumulation differ.

Based on the comparative graph of maximum compressive stress at the top fiber during the construction stages (Stage 1 to Stage 21), it is evident that the stress values produced by the Eurocode-based model are consistently higher than those of AASHTO and IRC, particularly in the early phases of segment additions. AASHTO results fall between those of Eurocode and IRC, while IRC consistently yields the lowest stress values across nearly all construction stages. These variations in stress values can be attributed to the technical aspects inherent to each design standard, particularly in the treatment of long-term concrete material behavior (time-dependent behavior), such as creep and shrinkage. Eurocode

employs a more detailed and comprehensive approach, specifically the CEB-FIP 1990 model, which considers various environmental parameters such as relative humidity, temperature, cement type, and loading age. This approach tends to produce higher stress redistributions, especially during the early stages of formwork release, resulting in greater recorded stresses. Conversely, AASHTO LRFD, which adopts an ACI-based model, utilizes simpler formulas with more conservative assumptions regarding elastic modulus and prestress losses. This leads to slightly lower stress values compared to Eurocode. Meanwhile, IRC (IRC:112-2011) uses a more empirical and conservative approach in calculating the effects of creep and shrinkage. In this simulation, the assumption of concrete age at initial loading being 3 days for the IRC model also contributes to higher shrinkage effects and long-term prestress losses, thus producing lower stress values than the other two codes. Another contributing factor lies in the calculation of initial prestress losses and stress redistribution due to tendon relaxation and concrete deformation. Eurocode allows a more aggressive calculation of effective prestress values, resulting in higher initial compressive stresses. On the other hand, IRC tends to produce lower results due to its more conservative consideration of prestress losses and its linear approach to time-dependent effects.

As shown in Table 3, Eurocode's more refined modeling of environmental and material factors explains the higher stress concentrations. This comparative matrix supports the observed divergence in structural response.

Table 3. Comparison of Time-Dependent Parameters Across Design Codes

Parameter	Eurocode (EN 1992-2)	AASHTO LRFD	IRC:112-2011
Shrinkage coefficient ε_{sh}	~2.5×10^{-4}	~2.0×10^{-4}	~1.8×10^{-4}
Creep coefficient φ	1.8 – 2.3 (variable)	1.4 – 1.8 (empirical)	~1.2 – 1.5
Notional member size	Detailed calc. ($h/2\beta$)	Approximate / constant	Section area/perimeter
Cement type factor	Explicitly defined	Not used explicitly	Not used explicitly
Relative humidity factor	Integrated in model	Often ignored	Not modeled

A deeper comparison of the time-dependent modeling assumptions reveals that Eurocode applies the CEB-FIP 1990 model, which includes higher shrinkage coefficients (e.g., $\varepsilon_{sh} \approx 2.5 \times 10^{-4}$ for 50 MPa concrete) compared to AASHTO ($\varepsilon_{sh} \approx 2.0 \times 10^{-4}$) and IRC ($\varepsilon_{sh} \approx 1.8 \times 10^{-4}$). Additionally, Eurocode considers a humidity correction factor and member notional size with more granularity, which amplifies creep effects. The creep coefficient (φ) for Eurocode can reach values above 2.0 under 70% relative humidity, while AASHTO typically limits it to around 1.8, and IRC applies a simplified empirical value around 1.5. These differences drive more aggressive stress redistributions in Eurocode, resulting in higher compression stress peaks, especially in early segmental additions.

From an engineering perspective, overestimating compressive stress by 10%—as observed in the Eurocode case—could lead to unnecessary increases in concrete grade or tendon force selection, resulting in higher material cost without proportional safety gain. However, this may also improve long-term crack control and serviceability. Conversely, underestimating stress, as in the IRC case, could increase the risk of service-level cracking or unexpected deflections. Therefore, understanding each code's safety philosophy is essential when adapting it to local conditions.

Overall, the differences in stress values among the standards are due to the varying complexity and conservatism in addressing the viscoelastic properties of materials, environmental conditions, and structural design parameters throughout the staged construction process. This highlights the importance of selecting an appropriate design code based on the context of the structure, climatic conditions, and the safety philosophy adopted in a segmental bridge construction project.

Eurocode produces the highest compressive stresses primarily due to the CEB-FIP 1990 model's detailed consideration of notional member size, environmental humidity, and cement type. It also assumes relatively lower creep recovery and includes humidity-dependent shrinkage strain

amplification. These factors collectively increase the calculated internal forces, particularly during early segment releases.

AASHTO adopts a more conservative but simplified modeling strategy, drawing on ACI-based approximations. It assumes uniform shrinkage and linear creep functions, which dampen the redistribution of stress over time. As a result, the internal force development is more gradual, producing moderate values between Eurocode and IRC.

IRC provides the lowest stress values because its creep and shrinkage models are largely empirical and based on simplified age factors without humidity correction. While this reduces complexity, it also underestimates the true time-dependent behavior, which could affect long-term performance prediction.

A stress summary for each code is provided in Tables 4 and 5.

Table 4. Maximum stress at the top fiber

Stage	Compression (kPa)			Tension (kPa)		
	AASHTO	EN	IRC	AASHTO	EN	IRC
Stage 1	0	0	0	92	68.28	72.53
Stage 2	3788	3786	3778	0	0	0
Stage 3	5146	5148	5126	0	0	0
Stage 4	6413	6421	6378	0	0	0
Stage 5	7515	7537	7462	0	0	0
Stage 6	8472	8512	8399	0	0	0
Stage 7	9296	9357	9199	0	0	0
Stage 8	9977	10060	9855	0	0	0
Stage 9	10520	10640	10380	0	0	0
Stage 10	10970	11120	10790	0	0	0
Stage 11	11290	11470	11080	0	0	0
Stage 12	11470	11690	11240	0	0	0
Stage 13	11550	11810	11280	0	0	0
Stage 14	10910	11220	10620	0	0	0
Stage 15	10160	10520	9853	0	0	0
Stage 16	9347	9759	9014	0	0	0
Stage 17	8437	8906	8082	0	0	0
Stage 18	7432	7959	7053	0	0	0
Stage 19	7870	8535	7613	163	171.3	181.8
Stage 20	8576	9054	8133	819	644.4	841.3
Stage 21	8584	9051	8132	642.5	509.5	684

Table 5. Maximum Stress at the bottom fiber

Stage	Compression (kPa)			Tension (kPa)		
	AASHTO	EN	IRC	AASHTO	EN	IRC
Stage 1	107	92.28	98.02	0	0.72	0.76
Stage 2	0	0	0	980	951.2	946.3
Stage 3	0	0	0	1165	1174	1156
Stage 4	0	0	0	1246	1267	1227
Stage 5	0	0	0	1128	1168	1095
Stage 6	0	0	0	858	913	843.1
Stage 7	296	6.95	170.1	827	842.6	813.7
Stage 8	874	536.1	757.2	817	821.2	811.1
Stage 9	1559	1192	1478	805	808.2	797.8
Stage 10	2339	1961	2319	793	797.7	786.7
Stage 11	3217	2846	3281	788	792.8	781.1
Stage 12	4213	3869	4387	719	724.7	712.4
Stage 13	5372	5000	5608	692	704.4	691.5
Stage 14	6853	6419	7121	462	468.2	455.4
Stage 15	8444	7945	8746	215	215.1	215.1
Stage 16	10140	9573	10480	232.6	232	232.3
Stage 17	11960	11320	12330	231	230.5	230.5
Stage 18	13930	13230	14240	232.4	231.9	231.9
Stage 19	16020	15270	16520	226.8	225.9	225.9
Stage 20	18760	18140	18920	1224	1170	1260
Stage 21	18450	17890	18630	1248	1189	1282

4. Conclusion

This study conducted a comparative construction stage analysis of a balanced cantilever bridge using three international design codes—AASHTO, Eurocode, and IRC—implemented in MIDAS Civil. The simulation results show that while all three codes exhibit similar stress development trends, their magnitudes vary significantly due to differences in how time-dependent effects such as creep, shrinkage, and prestress losses are modeled. Eurocode produced the highest compressive stresses due to its detailed environmental and material modeling (CEB-FIP), AASHTO followed with moderate results based on simplified ACI-based models, and IRC yielded the lowest values due to conservative and empirical assumptions.

From an engineering standpoint, these variations have significant implications. Overestimating compressive stress, as seen in Eurocode, could lead to conservative designs and increased material costs, while underestimating stress in IRC may risk serviceability issues. Therefore, careful code selection is necessary, especially in the context of Indonesia's growing infrastructure demands and ongoing efforts to update its national bridge design standards.

For Indonesian engineers, this study recommends adopting a hybrid approach. Eurocode offers greater accuracy in capturing long-term behavior and is suitable for large-scale or high-risk projects where precision is critical. AASHTO, on the other hand, provides a practical balance between safety and simplicity and may be better suited for general applications or when computational resources are limited. Integrating key elements from both codes into a revised SNI (Indonesian National Standard), particularly in modeling creep and shrinkage, would enable safer and more cost-effective designs tailored to local conditions.

This research has certain limitations. It does not account for temperature effects, dynamic loading (such as seismic or traffic vibration), or geometric imperfections. All material properties and environmental conditions were kept uniform across models, and no field validation was performed.

Future research should include full parametric analysis and calibration using site-specific monitoring data to enhance the robustness and local applicability of the findings.

Declaration of AI and AI-assisted technologies in the writing process

During the preparation of this manuscript, the authors used Editage, Grammarly, and ChatGPT as AI-assisted language-editing tools to improve grammar, clarity, and readability. The tool was not used to generate research data, perform numerical analysis, or replace the authors' scientific judgment. After using this tool, the authors reviewed, verified, and edited the content as needed and take full responsibility for the content of the publication.

Declaration of Competing Interest

The authors declare that they have no known competing financial interests or personal relationships that could have appeared to influence the work reported in this paper.

Acknowledgements

The authors gratefully acknowledge financial support from the Institut Teknologi Sepuluh Nopember for this work, under the project scheme of the Publication Writing and IPR Incentive Program (PPHKI) 2025.

References

[1] M. Gautam, "Bridge loadings of different countries in the context of Nepal," *M.S. thesis*, Department of Structural Engineering, Institute of Engineering, Pulchowk Campus, Tribhuvan University, Lalitpur, Nepal, 2000.

[2] R. M. Barker and J. A. Puckett, *Design of Highway Bridges: An LRFD Approach*, 4th ed. Hoboken, NJ, USA: John Wiley & Sons, 2021. DOI: https://doi.org/10.1002/9781119642534

[3] G. Jitha and C. Rajamallu, "Girder design of a balanced cantilever bridge with analysis using MIDAS Civil," *International Journal of Innovative Research in Advanced Engineering*, vol. 3, no. 6, p. 49, 2016. DOI: https://doi.org/10.6084/m9.figshare.3468842.v1

[4] Y. S. Patil and S. B. Shinde, "Comparative analysis and design of box girder bridge sub-structure with two different codes," *International Journal of Advanced Research in Engineering and Technology*, vol. 4, no. 5, pp. 134–139, 2013.

[5] A. Seni, "Comparison of live loads used in highway bridge design in North America with those used in Western Europe," in *Second International Symposium on Concrete Bridge Design*, Chicago, IL, USA, Apr. 1969. Detroit, MI, USA: American Concrete Institute, 1971, pp. 1–34.

[6] P. K. Thomas, "The evolution of a new highway bridge loading standard for India," *Indian Roads Congress Journal*, vol. 36, no. 2, pp. 147–185, Nov. 1975.

[7] A. C. Agarwal and M. S. Cheung, "Development of loading-truck model and live-load factor for the Canadian Standards Association CSA-S6 code," *Canadian Journal of Civil Engineering*, vol. 14, no. 1, pp. 58–67, 1987. DOI: https://doi.org/10.1139/l87-008

[8] S. B. Bhat, "Development of highway bridge loading for Nepal," *M.S. thesis*, Department of Structural Engineering, Institute of Engineering, Pulchowk Campus, Tribhuvan University, Lalitpur, Nepal, 2004.

[9] I. G. Buckle, "Overview of seismic design methods for bridges in different countries and future directions," *Technical report*, Department of Civil Engineering, State University of New York at Buffalo, Buffalo, NY, USA, 1996.

[10] J. P. Wacker and J. Groenier, "Comparative analysis of design codes for timber bridges in Canada, the United States, and Europe," *Transportation Research Record*, no. 2200, pp. 163–168, 2010. DOI: https://doi.org/10.3141/2200-19

[11] M. Okahara, J. Fukui, M. Nishitani, and K. Matsui, "Comparison of performance required by bridge design codes in various countries," in *Proceedings of the International Workshop on Life-Cycle Cost Analysis and Design of Civil Infrastructure Systems*, National Institute of Standards and

Technology Special Publication 1000-1, 2001, pp. 297–312.
[12] P. G. Buckland and R. G. Sexsmith, "A comparison of design loads for highway bridges," *Canadian Journal of Civil Engineering*, vol. 8, no. 1, pp. 16–21, 1981. DOI: https://doi.org/10.1139/l81-003
[13] V. K. Raina, *Concrete Bridge Practice: Analysis, Design and Economics*, 2nd ed. New Delhi, India: Tata McGraw-Hill, 1994, pp. 1–788.
[14] K. S. Rajagopalan, "Comparison of loads around the world for design of highway bridges," in *Second International Symposium on Concrete Bridge Design*, Chicago, IL, USA, Apr. 1969. Detroit, MI, USA: American Concrete Institute, 1971, pp. 35–48.
[15] W. I. W. A. Kamal, "Comparison of bridge design in Malaysia between American codes and British codes," *Ph.D. dissertation*, Universiti Teknologi Malaysia, Johor Bahru, Malaysia, 2005.
[16] H. Y. Aziz and J. Ma, "Design and analysis of bridge foundation with different codes," *Journal of Civil Engineering and Construction Technology*, vol. 2, no. 5, pp. 101–118, May 2011.
[17] D. Kamde, B. John, and A. Hulagabali, "Comparative study for the design of single-span bridge using AASHTO LRFD and Indian Standard method," *IOSR Journal of Mechanical and Civil Engineering*, pp. 40–44, 2014.
[18] R. J. Nielsen and E. R. Schmeckpeper, "Single-span prestressed girder bridge: LRFD design and comparison," *Journal of Bridge Engineering*, vol. 7, no. 1, pp. 22–30, 2002. DOI: https://doi.org/10.1061/(ASCE)1084-0702(2002)7:1(22)
[19] American Association of State Highway and Transportation Officials (AASHTO), *AASHTO LRFD Bridge Design Specifications*, 10th ed. Washington, DC, USA: AASHTO, 2024.
[20] American Association of State Highway and Transportation Officials (AASHTO), *AASHTO LRFD Bridge Design Specifications*, 9th ed. Washington, DC, USA: AASHTO, 2020.
[21] Fédération Internationale du Béton (fib), *CEB-FIP Model Code 1990*. Lausanne, Switzerland: fib, 1993.
[22] European Committee for Standardization, *Eurocode 1: Actions on Structures – Part 2: Traffic Loads on Bridges*, EN 1991-2. Brussels, Belgium: CEN, 2003.
[23] European Committee for Standardization, *Eurocode 2: Design of Concrete Structures – Part 2: Concrete Bridges*, EN 1992-2. Brussels, Belgium: CEN, 2005.
[24] Indian Roads Congress, *Standard Specifications and Code of Practice for Road Bridges: Section II – Loads and Stresses*, IRC:6-2000, 4th rev. New Delhi, India: Indian Roads Congress, 2000.
[25] Indian Roads Congress, *Standard Specifications and Code of Practice for Road Bridges: Section III – Cement Concrete (Plain and Reinforced)*, IRC:21-2000, 3rd rev. New Delhi, India: Indian Roads Congress, 2000.
[26] Indian Roads Congress, *Code of Practice for Concrete Road Bridges*, IRC:112-2011. New Delhi, India: Indian Roads Congress, 2011.
[27] Bureau of Indian Standards, *Plain and Reinforced Concrete – Code of Practice*, IS 456:2000. New Delhi, India: Bureau of Indian Standards, 2000.